Plant Mol Biol (2010) 74:47–59
DOI 10.1007/s11103-010-9653-0

The *Arabidopsis* chloroplast ribosome recycling factor is essential for embryogenesis and chloroplast biogenesis

Liyuan Wang · Min Ouyang · Qiannan Li · Meijuan Zou · Jinkui Guo · Jinfang Ma · Congming Lu · Lixin Zhang

Received: 18 January 2010 / Accepted: 19 May 2010 / Published online: 4 June 2010

Abstract To gain insight into the functions of the nuclear-encoded factors involved in chloroplast development, we characterized the *high chlorophyll fluorescence* and *pale green mutant 108-1* (designated as *hfp108-1*) of *Arabidopsis thaliana*. Map-based cloning revealed that the mutant contains a tandem repeat of part of the sequence (including 116 nucleotides from 631 to 746 bp downstream of the ATG) of *At3g63190*, which encodes a chloroplast ribosome recycling factor homologue and was named AtcpRRF. The chloroplasts of *hfp108-1* plants contain few internal thylakoid membranes and are severely defective in the accumulation of chloroplast-encoded proteins. In vivo labeling experiments showed a drastic decrease in the synthesis of the chloroplast-encoded proteins, which may be attributed primarily to reduced translation of the corresponding mRNA molecules. The level of the *HFP108* transcript was greatly reduced in *hfp108-1*, so *hfp108-1* showed a weak phenotype, and null alleles of *HFP108* (*hfp108-2*) were embryonic lethal. Observations with cleared seeds in the same silique showed that homozygous *hfp108-2* seeds were blocked at the heart stage and did not develop further. Thus, these results suggest that AtcpRRF is essential for embryogenesis and chloroplast biogenesis.

Keywords *Arabidopsis* · Chloroplast biogenesis · Embryogenesis · Ribosome recycling factor · Translation

L. Wang · M. Ouyang · Q. Li · M. Zou · J. Guo · J. Ma · C. Lu · L. Zhang (✉)
Photosynthesis Research Center, Key Laboratory of Photobiology, Institute of Botany, Chinese Academy of Sciences, 100093 Beijing, China
e-mail: zhanglixin@ibcas.ac.cn

Introduction

Chloroplasts have their own translation system, although the chloroplast genomes of higher plants retain less than 100 genes and more than 90% of their genome has been transferred to the nucleus during evolution (Sato et al. 1999; Ahlert et al. 2003; Abdallah et al. 2000). The plant chloroplast translation system is known to be similar to the prokaryotic translation system (Sugiura 1992; Zerges 2000). However, the chloroplast translation system has several unusual features. For example, chloroplast mRNAs do not have an m7G cap and can be present as polycistronic transcripts (Sugita and Sugiura 1996; Rochaix 1996). Several chloroplast protein synthesis factors, such as elongation factor G (EF-G) (Hernandez-Torres et al. 1993; Akkaya et al. 1994; Albrecht et al. 2006; Ruppel and Hangarter 2007), ribosome recycling factor (RRF) (Rolland et al. 1999), initiation factor 1 (IF1) (Hirose et al. 1999), initiation factor 2 (IF2) (Campos et al. 2001), peptide chain release factor 2 (RF2) (Meurer et al. 1996a, 2002), and chloroplast ribosome release factor 1(RF1) (Motohashi et al. 2007), have been identified in higher plants.

Ribosome recycling factor (RRF) was first discovered in *Escherichia coli* (*E. coli*) (Hirashima and Kaji 1970), and its corresponding gene was subsequently cloned (Ichikawa and Kaji 1989). In bacteria, protein synthesis consists of four steps: initiation, elongation, termination, and recycling of ribosomes for the next round of translation. After termination of translation, the 70S ribosomes, which are the working form of the ribosome, have to be recycled for initiation of the next round of protein synthesis by dissociation into subunits. The recycling step involves the disassembly of the post-termination complex, which is catalyzed by the cooperative action of three translation factors: ribosome recycling factor (RRF), elongation factor

G (EF-G), and initiation factor 3 (IF3) (reviewed in Kaji et al. 2001). RRF and EF-G alone transiently dissociate 70S ribosomes. Subsequently, the dissociation is stabilized by IF3, which binds to the transiently formed 30S subunits and prevents re-association into 70S ribosomes. The stable dissociation of ribosomes into subunits through the cooperation of the three factors completes the ribosome cycle, and the resulting subunits are ready for the next round of translation (Hirokawa et al. 2005). RRF is essential for bacteria and inactivation of RRF is bactericidal or bacteriostatic (Janosi et al. 1994, 1998).

Homologues of the RRF gene (*frr*) have been identified in the prokaryotic genomes that have been sequenced, except for *Archaea* (reviewed in Kaji et al. 1998; Janosi et al. 1996; Bult et al. 1996). An *frr* homologue gene was also found in the nuclear genome of spinach (*Spinacia oleracea* L.) and its encoded protein product was localized in the chloroplast (Rolland et al. 1999). However, compared with bacterial ribosome recycling factors, the biological functions of the chloroplast homologues of RRF in vivo have not been characterized. In this study, we report the identification of an *Arabidopsis* mutant with a high chlorophyll fluorescence and pale green phenotype, which was termed *hfp108-1*. *HFP108* encodes a chloroplast ribosome recycling factor (cpRRF). Physiological analysis of the mutant revealed that HFP108 has an important function in chloroplast biogenesis and plays an essential role in translation in plastids. Null alleles of *HFP108* were also embryonic lethal. Our results indicated that cpRRF is essential for chloroplast function and viability of *Arabidopsis*.

Materials and methods

Plant material and growth conditions

The high chlorophyll fluorescence *hfp108-1* mutant was isolated from a collection of pSKI015 T-DNA-mutagenized *Arabidopsis thaliana* (ecotype *Columbia*) lines from the *Arabidopsis* Biological Resource Center (ABRC) (Weigel et al. 2000) using a chlorophyll fluorescence imaging system (Ma et al. 2007). The T-DNA insertion line, Salk_102361 was obtained from the ABRC, and the T-DNA was inserted into exon 8 of *At3g63190*. The heterozygous plant was verified by PCR using the primers *hfp108-2*-LP (5′-GATTGTTGAATTACGTCTCC-3′) and *hfp108-2*-RP (5′- TGACCCCTAATAACGATG-3′). The T-DNA insertion was confirmed by PCR analysis and subsequent sequencing with the primers T-DNA-LB (5′-ATTTTGC CGATTTCGGAAC-3′) and *hfp108-2*-RP. Wild-type and mutant seedlings were grown on Murashige and Skoog (MS) medium containing 3% sucrose under short-day conditions (10-h light/14-h dark cycle) with a photon flux density of 120 μmol m^{-2} s^{-1} at 22°C.

Chlorophyll fluorescence analysis

Chlorophyll fluorescence was measured with a PAM-2000 portable chlorophyll fluorometer (Walz) connected to leaves which had been dark-adapted for 30 min before measurements, with a leaf-clip holder (model 2030-B; Walz). The minimum fluorescence yield (*Fo*) was measured under 650 nm light with a very low intensity (0.8 μmol m^{-2} s^{-1}). A saturating pulse of white light (3000 μmol m^{-2} s^{-1} for 1 s) was used to estimate the maximum fluorescence yield (*Fm*), and the ratio of variable (*Fv*) to maximum (*Fm*) fluorescence [$Fv/Fm = (Fm - Fo)/Fm$] was calculated basically according to Meurer et al. (1996b). All of the measurements described above were performed in a dark room with stable ambient conditions.

Transmission electron microscopy

Transmission electron microscopy analysis was performed essentially as described by Peng et al. (2006). The wild-type and mutant rosette leaves were collected, cut into small pieces, and fixed in 2.5% glutaraldehyde in phosphate buffer for 4 h at 4°C. After fixation, the samples were post-fixed in 1% OsO4 overnight at 4°C, dehydrated in an ethanol series, infiltrated with a graded series of epoxy resin in epoxy propane, and embedded in Epon 812 resin. Thin sections were obtained using a diamond knife on a Reichert OM2 ultramicrotome, stained in 2% uranyl acetate at pH5.0, and then in 10 mM lead citrate at pH12, and viewed with a transmission electron microscope (JEM-1230; JEOL).

Map-based cloning and complementation

The *hfp108-1* mutation was mapped based on the polymorphisms between two *Arabidopsis* ecotypes, *Columbia* and *Landsberg erecta* (Lukowitz et al. 2000). The mapping population was obtained by crossing wild-type plants of the ecotype *Landsberg erecta* with the mutant plants (*Columbia*). Three hundred and sixty-eight homozygous F2 mutant plants (*hfp108*/*hfp108*) were obtained based on the high chlorophyll fluorescence phenotype, and their genomic DNA was extracted and examined by PCR with specific molecular markers. The linkage group of the *hfp108* mutation was determined with a series of simple sequence length polymorphism markers. The region of the mutation locus was determined to be within the region between the bacterial artificial chromosome T20O10 and the end of the lower arm of chromosome 3. Candidate genes with a predicted chloroplast transit peptide in this region were

sequenced and analyzed with genomic DNA from *hfp108-1* and wild-type plants (*Columbia*). For complementation of the *hfp108-1* phenotype, a fragment containing the full-length *hfp108* coding sequence was amplified with the following primers: 5′-TCTAGAATGGCGGCTTCTTTCT CTTCCAC-3′ and 5′-GTCGACTCACACCTTCATCAAT TCC-3′. The PCR product was cleaved with *Xba*I and *Sal*I and subcloned into the pBI121 vector under the control of the cauliflower mosaic virus 35S promoter. Subsequently, the construct was transferred to heterozygous *hfp108-1* plants by *Agrobacterium tumefaciens*-mediated transformation by the floral dip method (Clough and Bent 1998). Transgenic plants were selected on MS medium containing 40 μg μL^{-1} kanamycin monosulfate and grown in a greenhouse to produce seeds for PCR analysis. The primers used for the identification of homozygous *hfp108-1* are: 5′-GTACAGAAAACCATTAGC-3′ and 5′-AACGATTTG GATGTGATT-3′. The success of the complementation was confirmed by chlorophyll fluorescence analysis.

RT-PCR analysis

Total RNA extracted from leaves of the *hfp108-1* mutant and wild-type plants was treated with DNase I and then reverse transcribed with Oligo(dT) (Takara). For the determination of *At3g63190* expression, RT-PCR was performed from the cDNA above using a set of specific primers for the *At3g63190* gene that encompassed the mutation site in *hfp108-1*. The primers used were as follows: sense (5′-CAAATCCTTCACGTTGTC-3′), and antisense (5′-GA AGAAATAGAAGCAGAG-3′). To ensure that there was an equal amount of RNA in each sample, RT-PCR analysis of the *actin11* cDNA was performed using the following primers: sense (5′-AACTGGGATGATATGGAGAA-3′) and antisense (5′-CCTCCAATCCAGACACTGTA-3′).

GFP fusion constructs for transient expression in protoplasts

A fragment encoding the N-terminal 117 amino acids of HFP108 was amplified by RT-PCR with the primers 5′-GTCGACATGGCGGCTTCTTTCTCTTCC-3′ and 5′-C CATGGTTATGGAGTTGAAACTCGTCC-3′ and subcloned into the pUC18-35s-sGFP vector to generate a fusion protein with GFP in the C-terminus. The fragments containing the N-terminal part (1-282 amino acids) of AtFbr1 and the transit peptide (1-81 amino acids) of the small subunit of ribulose bisphosphate carboxylase were amplified using the primer pairs 5′-ACAACTCGAGAT GAGACCCCCAGTTACAGG-3′ and 5′-TCCATGGTCA CCTGTTCTGCTGGCTTAAAC-3′ and 5′-CACGTCGAC AAACCTCAGTCACACAAAGAG-3′ and 5′-TCCATGG ATTCGGAATCGGTAAGGTCAGG-3′, respectively, which were subcloned into the pUC18-35s-sGFP vector and used as nuclear and chloroplast controls, respectively. The resulting constructs and the negative control vector without additional coding sequence were introduced into wild-type *Arabidopsis*. The GFP emission was detected using a 505–530 nm bandpass filter following excitation of the samples with a 488 nm laser (Cai et al. 2009).

Northern blot analysis

Northern blot analysis was performed basically as described in Sambrook and Russell (2001). Total RNA isolated from the wild-type and mutant plants was fractionated, transferred onto nylon membranes, and subsequently probed with ^{32}P-labeled cDNA probes. Following high-stringency hybridization and washing, blots were exposed to x-ray film for 1–3 days. The hybridization probes were prepared using a random priming labeling kit (Promega, USA) with PCR fragments of the encoding regions of the target genes. The sequences of the PCR primers used to amplify the genes are presented in Table 1.

Polysome analysis

Polysome analysis was carried out according to Barkan (1998). Leaf tissue was ground to a fine powder in liquid nitrogen, and polysome extraction buffer was then added. After centrifugation, the supernatant (0.5 mL) was layered onto 15–55% sucrose gradients and centrifuged for 65 min

Table 1 Primers used for the preparation of the hybridization probes

Gene	Sense primer	Antisense primer
psbA	5′-TTATCCATTTGTAGATGGAGCCTCA-3′	5′-ATGACTGCAATTTTAGAGAGACGCG-3′
psbB	5′-GCAAGGATCCATGGGTTTGCCTTGG-3′	5′-GCAACTCGAGATCAGACTGCTTGTCG-3′
psbD	5′-CTGGTCTATTGCTCTTTCCTTGTGCCTAT-3′	5′-GCCGCCATCCAAGCACGAATACCTT-3′
psaA	5′-CAATTGGCGCATTGGTCTTCGCAG-3′	5′-GTGCTCGCTGTTTCACCAGGGGCTG-3′
cab	5′-CTTTGTGCTGCACTACTCAACC-3′	5′-CGATGGCTTGAACGAAGAATCC-3′
psbO	5′-AACTTCCTCGGCTCGCCTCACT-3′	5′-CTCCTCGTCTCCTCTGCCTCC-3′

at 45,000 rpm at 4°C in a SW55Ti rotor (Beckman, Munich, Germany). Fractions of equal volume were collected, and RNA was extracted from each fraction and then subjected to RNA gel hybridization.

Antiserum production

For production of polyclonal antibodies against HFP108, a cDNA fragment encoding part of HFP108 (amino acids 19–274) was amplified by PCR using the primers 5′-GG ATCCGCCAACTACTCCAAGCCTC-3′ and 5′-CCGTCG ACCACCTTCATCAATTCCTTTTC-3′. The PCR product was cleaved with *Bam*HI and *Sal*I and fused in-frame with the N-terminal His affinity tag of pET28a. BL21 cells were harvested after incubation with 0.6 mM isopropyl thiol-β-D-galactoside for 5 h. The overexpressed proteins were purified using a nickel affinity column, and polyclonal antibodies were raised in rabbits with purified antigen.

Microscopy of developing seeds

For the microscopy experiments, seeds were removed from heterozygous *hfp108-2* mutant siliques and cleared in Hoyer's solution (3.75 g of gum arabic, 50 g of chloral hydrate, and 2.5 mL of glycerol in 15 mL of water) as described in Meinke (1994). Cleared seeds were then examined by light microscopy (Zeiss Axioskop) using differential interference contrast (Chi et al. 2008).

In vivo labeling of chloroplast proteins

In vivo chloroplast protein labeling was performed essentially according to Meurer et al. (1998). Primary leaves of 12-day-old young seedlings were radiolabeled with 1 mCi/mL $^{[35S]}$Met (specific activity > 1000 Ci/mmol; Amersham Pharmacia Biotech) in the presence of 20 µg/mL cycloheximide for 20 min, followed by incubation in 20 µg/mL cycloheximide for 30 min at 25°C. After labeling, the leaves were washed twice with homogenization buffer (50 mM Tris–HCl, pH 7.5, 150 mM NaCl, and 2 mM EDTA) and ground with 300 µL of the same buffer. The membranes were pelleted by centrifugation at 15,000 g for 10 min and resuspended in 100 µL of homogenization buffer. The samples were solubilized and separated by SDS–PAGE, and the labeled proteins were visualized by autoradiography.

SDS–PAGE and immunoblotting

Total proteins were isolated and separated by SDS–PAGE according to Martínez-García et al. (1999). For immunoblot analysis, the resolved proteins were transferred onto nitrocellulose membranes that were incubated with specific primary antibodies, and the signals from the secondary conjugated antibodies were detected by the enhanced chemiluminescence method.

Results

Isolation of an *hfp108-1* mutant

The high-chlorophyll-fluorescence recessive mutant *hfp108-1* was isolated from the Scheible and Somerville T-DNA *Arabidopsis* lines (Weigel et al. 2000). The *Fv/Fm* values in 4-week-old leaves were 0.82 ± 0.02 and 0.23 ± 0.03 of the wild-type and *hfp108-1* mutant plants grown on agar plates with 3% sucrose, respectively. Growth of homozygous *hfp108-1* seedlings on sucrose-supplemented MS-media under a light intensity of 120 µmol m^{-2} s^{-1} was greatly reduced, and the leaves appeared pale green (Fig. 1). The mutant was seedling-lethal when grown on soil (data not shown).

Chloroplast development in *hfp108-1* is impaired

To investigate the effects of the *hfp108-1* mutation on chloroplast development, we analyzed the morphological changes in plastids in the 4-week-old leaves of wild-type and mutant plants by transmission electron microscopy (Fig. 2). Cells in wild-type plants contained numerous normal chloroplasts, in which well-developed thylakoid membranes were composed of grana connected by the stroma lamellae. In contrast, only plastids with rudimentary lamellar structures were observed in mature leaves of *hfp108-1* plants. The plastids in *hfp108-1* did not develop into normal mature chloroplasts with the thylakoid membrane system. The internal membranes in the mutant plastids were nonstacked, and grana and stroma thylakoids could not be distinguished. The plastids from the mutant were more spherical and significantly smaller than those in wild-type plants. In addition, assimilatory starch was not

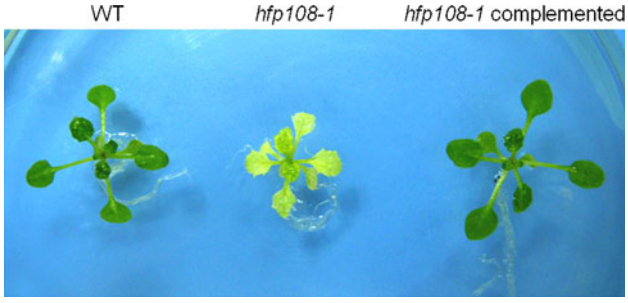

Fig. 1 Phenotype of 3-week-old wild-type, homozygous *hfp108-1* and *hfp108-1* complemented plants on Murashige and Skoog (1962) medium containing 3% sucrose

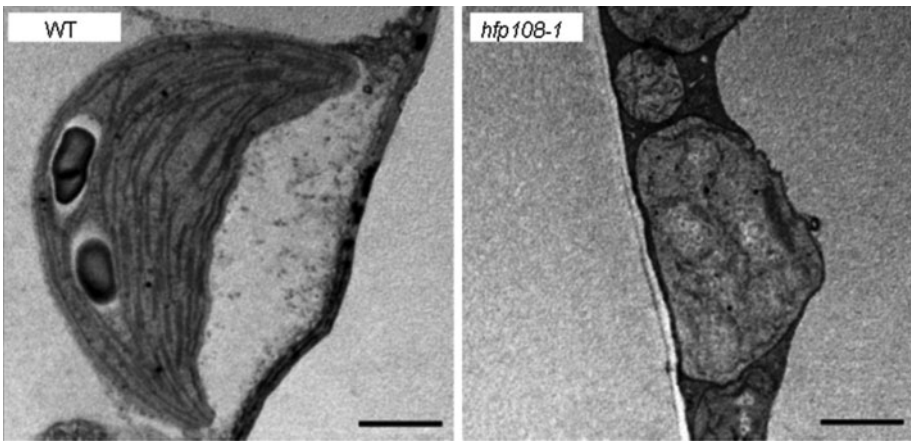

Fig. 2 Ultrastructures of plastids in the 4-week-old leaves of wild-type and *hfp108-1* mutant plants. *Bars* = 1 μm

detectable in *hfp108-1*. Thus, electron microscopy analysis showed that the plastids of *hfp108-1* were arrested in an early developmental stage without the typical stack of thylakoid membranes.

Molecular cloning of the *HFP108* gene

Genetic analysis revealed that the *hfp108-1* mutant phenotype did not cosegregate with the phosphinothricin resistance marker (data not shown), indicating that the mutated *HFP108* gene was not tagged by the T-DNA. Map-based cloning of the *hfp108-1* mutant using the simple sequence length polymorphism molecular markers ciw4 and nga6 and two newly developed markers (T20N10 and T20O10) revealed a nucleotide duplication (nucleotide positions 631–746 bp relative to the ATG codon) in the *At3g63190* gene (Fig. 3a). Reverse transcription (RT)-PCR analysis showed that the transcript levels of the *At3g63190* gene were drastically reduced in the *hfp108-1* mutant (Fig. 3b). Sequencing of the RT-PCR product derived from the mutant demonstrated that the *HFP108* transcript detected was correctly spliced in the mutant. Immunoblot analysis with an HFP108 antibody revealed that a small amount of HFP108 could be detected in total protein preparations of the *hfp108-1* mutant (Fig. 3c). An independent T-DNA insertion mutant line, Salk_102361 (containing a T-DNA insertion at nucleotide position 1,474 bp in exon 8 of the *At3g63190* gene downstream of the ATG codon) was obtained from the *Arabidopsis* Biological Resource Center (ABRC), which was hereafter referred to as *hfp108-2* .

To confirm that the mutation of the *At3g63190* gene was responsible for the mutant phenotype, complementation analysis was performed by introduction of the cDNA of *At3g63190* under the control of the 35S promoter into heterozygous *hfp108-1* plants by *Agrobacterium tumefaciens*-mediated transformation. In the progeny of these transformants, we identified five transgenic plants that were homozygous for the *hfp108-1* mutation. The transgenic plants exhibited a phenotype similar to wild-type plants (Fig. 1), and chlorophyll fluorescence induction measurements showed that the transgenic plants exhibited similar kinetics to wild-type plants (data not shown). Thus, the introduced cDNA of *At3g63190* was able to complement the *hfp108-1* mutant phenotype, and inactivation of the *At3g63190* gene was responsible for the *hfp108-1* mutant phenotype.

HFP108 is essential at an early stage of embryogenesis

Heterozygous *hfp108-2* mutants had a wild-type phenotype; however, there were no homozygous knockout plants. The segregation ratio of heterozygotes to wild type was 45:22 = 2.0:1 ($\chi^2 = 0.007$) and was close to the expected 2:1 ratio, which suggested that *HFP108* is essential during the early stages of seed formation and embryogenesis. Thus, we analyzed seeds in developing and mature siliques of heterozygous plants, respectively. As shown in Figs. 4a and b, siliques of heterozygous plants contained both white and green seeds, and seeds in developing siliques of wild-type plants were all green (Fig. 4a). Statistical analysis of the green and white seeds in several siliques showed that the segregation ratio was close to 3:1 (Table 2), which is consistent with single recessive alleles. In fully developed siliques, mutant seeds, which did not germinate, were small and shriveled and had a purple coloration compared with the wild-type seeds (Fig. 4b).

To identify at which stage of embryogenesis *hfp108-2* mutants were arrested, we further examined the embryos from these white and green seeds in the *hfp108-2* heterozygous mutant from a developmental series of siliques using interference contrast light microscopy. Observation with cleared seeds in the same silique confirmed that homozygous seeds were blocked at the heart stage and failed to

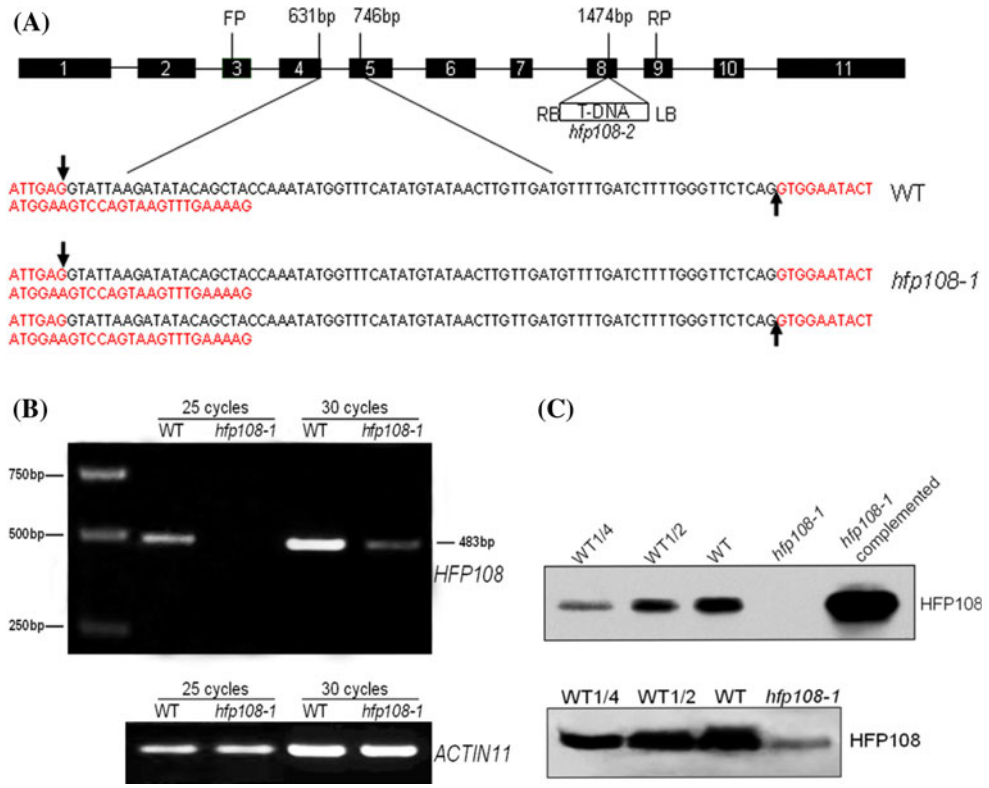

Fig. 3 Identification of the *hfp108-1* mutation. **a** The mutation site in the *hfp108-1* mutant and gene structure of *At3g63190*. The exons are shown as *black boxes*, and introns are shown as *black lines*. The *hfp108-1* mutation is based on a tandemly repeated sequence (including 116 nucleotides from 631 to 746 bp downstream of the ATG) of *At3g63190*. The *arrows* show the splicing site in the wild-type and *hfp108-1* genes. The base pairs in *red and black* represent exons and introns, respectively. The *hfp108-2* mutation is indicated. "LB" and "RB" represent the left and right borders, respectively, of the T-DNA insertion in the *hfp108-2* line. "FP" and "RP" represent the forward primer and the reverse primer, respectively, for *At3g63190* used in the RT-PCR analysis. **b** RT-PCR analysis of mutant plants. RT-PCR was performed with specific primers for the *hfp108* and *actin11* genes. **c** Immunodetection of HFP108 in WT, *hfp108-1* and the mutant complemented with HFP108 cDNA (*hfp108-1* complemented). The total protein preparations from WT, *hfp108-1* and complemented plants (20 μg, *upper*) and those from WT and *hfp108-1* (100 μg, *lower*) were separated by SDS–PAGE and the blots were probed with specific antibody against HFP108. WT, wild type

undergo the transition into the torpedo stage, whereas embryos in WT and heterozygous seeds underwent the well-defined developmental stages, such as globular, heart, torpedo, walking-stick and curled cotyledon (Fig. 4c).

HFP108 encodes a chloroplast-localized ribosome recycling factor homologue

The *HFP108* (*At3g63190*) gene contains 11 exons and encodes a protein of 275 amino acids. A homology search using the BLASTX program (http://www.ncbi.nlm.nih.gov/blast/) revealed that the HFP108 protein showed 67, 59, 44, and 37% identity with RRF-like proteins from *Oryza sativa* (Os07g0570700), *Synechococcus elongatus* (strain PCC6301), *Escherichia coli* (strain K-12 substrain MG1655) and *Arabidopsis* mitochondria (At3g01800), respectively. All of these proteins contained the RRF super family conserved domain (shown by the underline) (Fig. 5a). TargetP analysis suggested that HFP108 contains a typical N-terminal transit peptide for targeting to the chloroplast.

To determine the subcellular localization of the HFP108 protein, a fragment of the 117N-terminal amino acids of HFP108 was fused to the N-terminus of the synthetic GFP (sGFP) (Chiu et al. 1996). The HFP108-GFP fusion proteins were transiently expressed in protoplasts under the control of the cauliflower mosaic virus 35S promoter, and GFP fluorescence exclusively colocalized with the chloroplastic chlorophyll, in accordance with results obtained when GFP was fused to the transit peptide of the small subunit of ribulose bisphosphate carboxylase (Lee et al. 2002). When GFP was fused to the targeting signal of the fibrillarin protein from *Arabidopsis* (Pih et al. 2000), GFP signals were localized in the nucleus (Fig. 5b). In addition, GFP signals accumulated in both the cytoplasm and nucleus when *Arabidopsis* was transformed with the control vector without a specific targeting sequence. Thus, these results indicate that HFP108 is localized to the chloroplast.

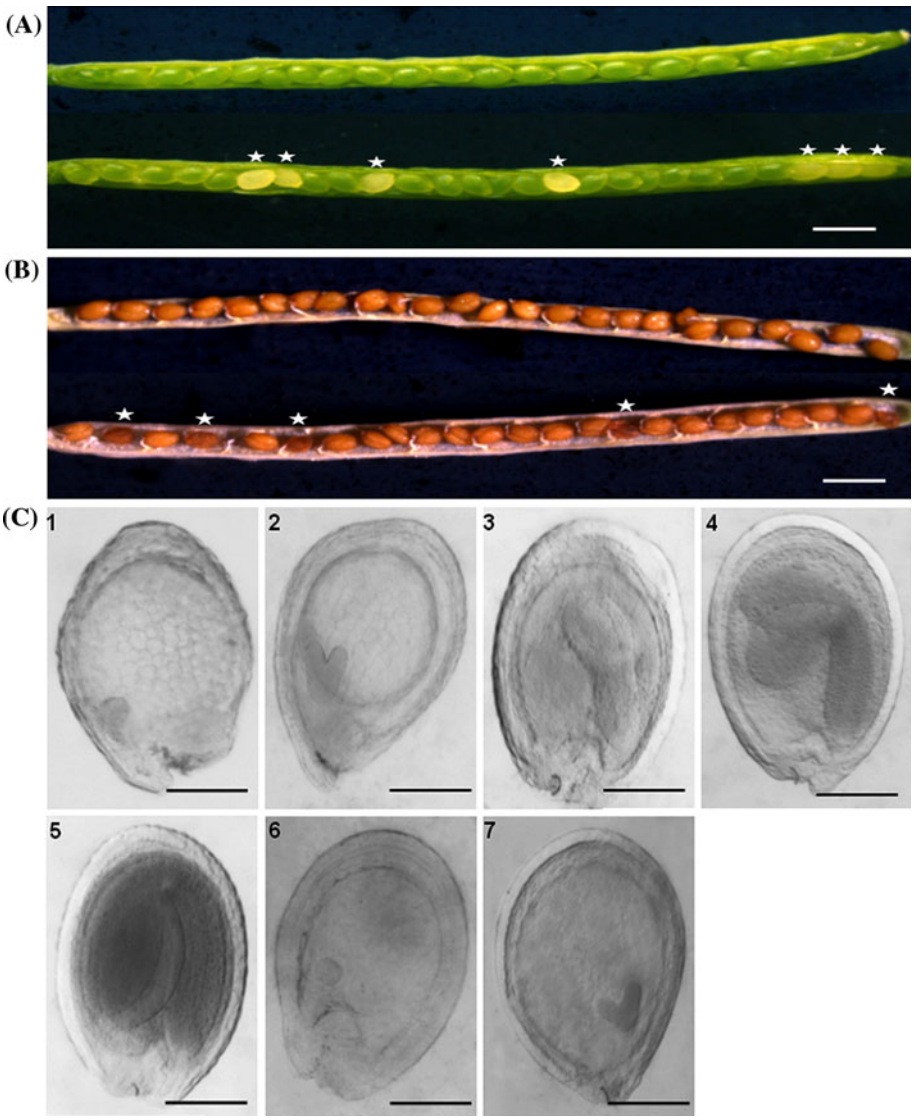

Fig. 4 Microscopy of developing embryos in siliques of wild-type and heterozygous *hfp108-2* plants. **a** Opened developing siliques of wild-type plants (*upper*) and heterozygous *hfp108-2* mutants (*lower*). Seeds in the developing siliques of wild type are all green, whereas the siliques of heterozygous mutant alleles have white (indicated by the *asterisks*) and green seeds with an average ratio of 1:3 (Table 2). *Bar* = 1 mm. **b** Opened mature siliques of wild-type plants (*upper*) and heterozygous *hfp108-2* mutants (*lower*). In the mature silique of heterozygous *hfp108-2* mutants, homozygous mutant seeds are recognizable as smaller, wrinkled and puce seeds, as indicated by the *asterisks*. *Bar* = 1 mm. **c** Nomarski bright-field microscopy of cleared seeds of the heterozygous *hfp108-2* mutant siliques. Embryo development of wild-type seeds at the globular (*1*), heart (*2*), torpedo (*3*), walking-stick (*4*) and cotyledon (*5*) stages and homozygous *hfp108-2* at the globular (*6*) and heart (*7*) stages. *Bars* = 100 μm

Table 2 Segregation analysis of the green and white seeds in developing siliques of heterozygous *hfp108-2*

Genotype	Green seeds	White seeds	Ratio	χ^2
+/*hfp108-2*	211	72	2.9:1	0.029

$\chi^2_{0.05,1} = 3.84$

The *hfp108-1* mutant fails to accumulate chloroplast-encoded proteins

Next we examined the abundance of chloroplast proteins in the *hfp108-1* mutant with specific antibodies (Fig. 6). Our results showed that the proteins D1 (encoded by *psbA*), D2 (encoded by *psbD*), CP43 (encoded by *psbC*), CP47 (encoded by *psbB*) and PsaA/B (encoded by *psaA/B*) encoded by plastid genes were barely detectable in *hfp108-1*. The levels of protein encoded by the nuclear gene *PsbO* reduced to ~30% of wild type, and LHCII (encoded by *cab*) accumulated to the normal wild-type level in *hfp108-1* mutants (Fig. 6). Hence, the immunoblot analysis showed a severe defect in the accumulation of chloroplast-encoded proteins in *hfp108-1*.

Expression of nuclear- and chloroplast-encoded genes in *hfp108-1*

The immunoblot analysis showed that the levels of photosynthetic proteins were decreased dramatically. To elucidate the effect of the *HFP108* mutation on the expression of photosynthetic genes, we analyzed the transcript levels of two nuclear-encoded genes, *psbO* and *cab*, and four chloroplast-encoded genes, *psbA*, *psbB*, *psbD* and *psaA/B*. In the *hfp108-1* plants, the levels of the *psbA*, *psbB*, *psbD* and *psaA/B* gene transcripts were decreased to

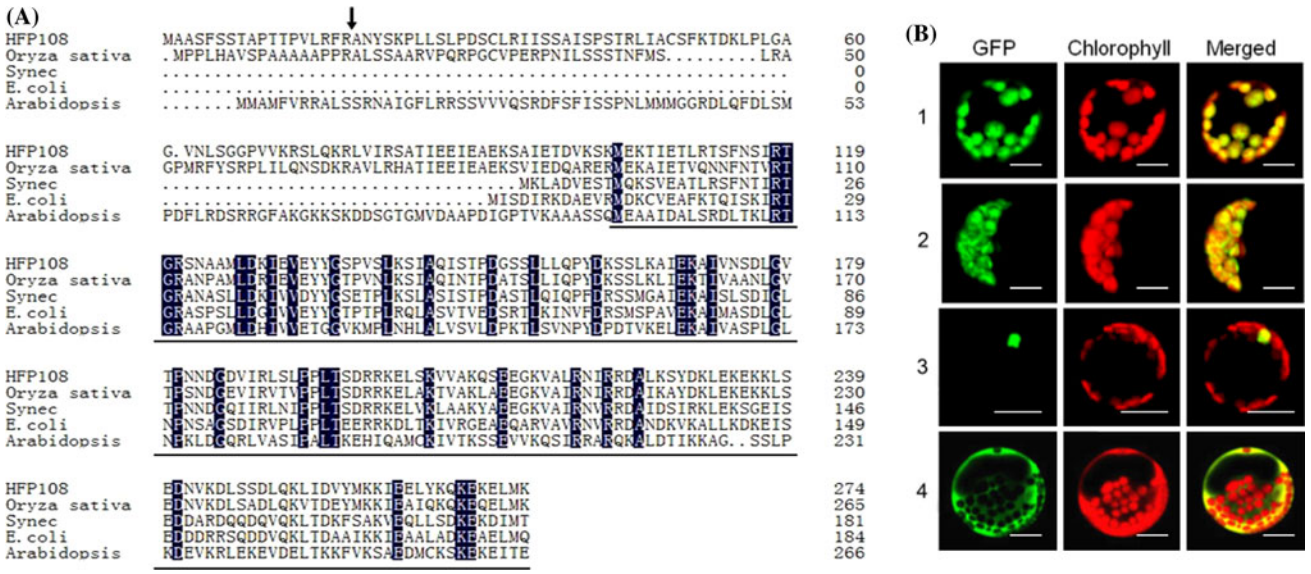

Fig. 5 HFP108 sequence alignment and subcellular localization. **a** Alignment of the deduced amino acid sequences from *Arabidopsis* HFP108 and RRF-like proteins of various species. The *arrow* is the putative cleavage site of the transit peptide in the HFP108 amino acid sequence. The *black boxes* indicate strictly conserved amino acids. The *underline* shows the RRF super family conserved domain. *Oryza sativa*, RRF in *Oryza sativa* (NP_001060047.1); *Synec*, RRF in *Synechococcus elongatus* (strain PCC6301); *E. coli,* RRF in *Escherichia coli*; *Arabidopsis*, another putative RRF (NP_186829.3) in *Arabidopsis thaliana*. **b** Subcellular localization of the HFP108 protein according to the fluorescence signals visualized using confocal laser scanning microscopy. *Green fluorescence* indicates GFP, *red fluorescence* shows chloroplast auto-fluorescence, and *orange/yellow fluorescence* shows regions where the two types of fluorescence colocalize. (*1*) GFP signals from the HFP108-GFP fusion protein. (*2*) Control with the transit peptide of the small subunit of ribulose bisphosphate carboxylase. (*3*) Control with the nuclear localization signal of fibrillarin. (*4*) Control lacking the transit peptide. *Bars* = 20 μm

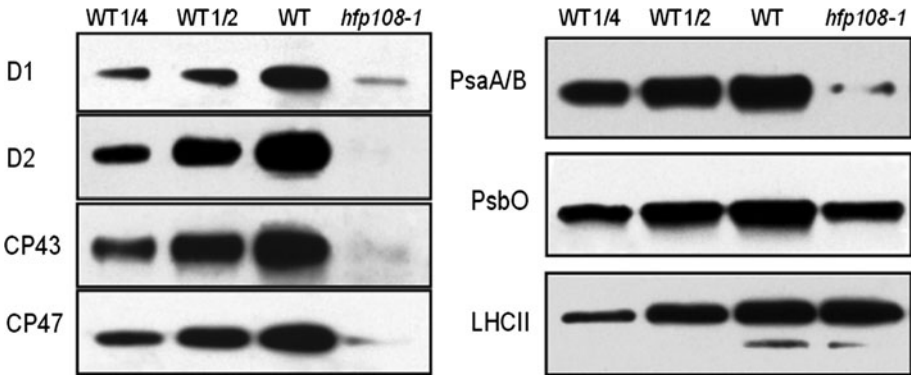

Fig. 6 Immunoblot analysis of chloroplast proteins from the wild-type and *hfp108-1* plants. Total protein (10 μg) was isolated from WT and *hfp108-1* and separated by SDS–PAGE. After gel electrophoresis, the resolved proteins were transferred to a nitrocellulose membrane and immunodetected with the specific antisera

approximately 50% of wild type, and levels of the *cab* and *psbO* transcripts were similar in both wild-type and *hfp108-1* plants (Fig. 7a).

Synthesis of plastid-encoded proteins is remarkably reduced in *hfp108-1*

To investigate whether the reduced accumulation of photosynthetic proteins was due to impaired translation in *hfp108-1* mutants, we in vivo labeled of chloroplast proteins with ^{35}S-Met in the presence of cycloheximide, which blocks the translation of nuclear-encoded proteins. After a 20-min pulse labeling, the levels of incorporation of ^{35}S-Met into PsaA/B, the α- and β-subunits of the chloroplast ATP synthase (CF1α/β), CP43, CP47, D1 and D2 were dramatically reduced compared with those in the wild-type plants (Fig. 7b).

Polysome association of chloroplast-encoded genes transcripts is altered in the *hfp108-1* mutant

To define the mutational defect in the mutant *hfp108-1* more precisely, we performed a ribosomal loading assay to determine whether the mutation in *hfp108* affects the ability of the *psbA* and *psbD* mRNAs to associate with polyribosomes. Polysomes were extracted and fractionated

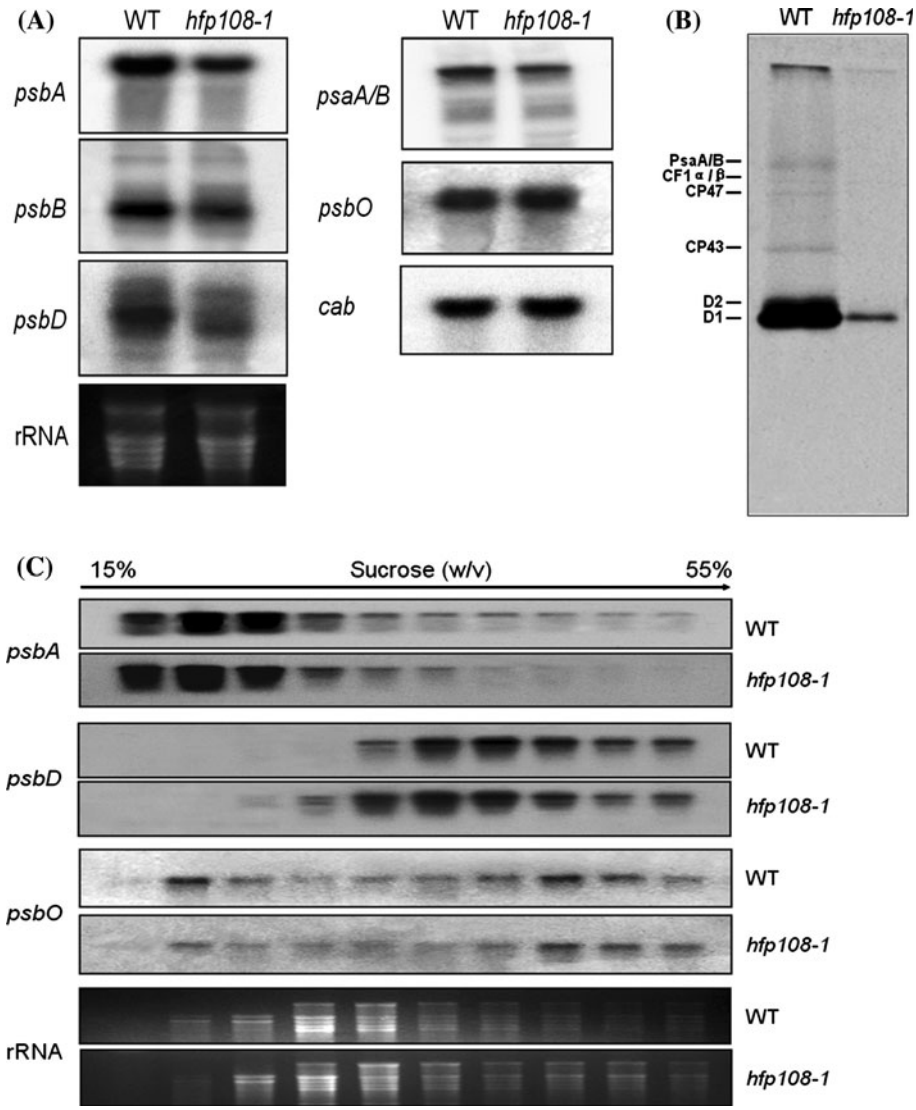

Fig. 7 mRNA expression and in vivo chloroplast protein synthesis analyses. **a** RNA gel blot hybridization with total RNA from the leaves of wild-type and *hfp108-1* plants. Total leaf RNA from 5-week-old wild-type and *hfp108-1* plants was size-fractionated by agarose gel electrophoresis, transferred to a nylonmembrane, and probed with ^{32}P-labeled cDNA probes for the *psbA*, *psbB*, *psbD*, *psaA/B*, *psbO* and *cab* genes. rRNA was visualized by staining with ethidium bromide as a loading control. **b** Pulse labeling of the thylakoid membrane proteins. After pulse labeling young *Arabidopsis* seedlings in the presence of cycloheximide for 20 min, thylakoid membranes were isolated, and the proteins were separated by SDS-urea-PAGE and visualized autoradiographically. **c** Polysome loading of the *psbA*, *psbD* and *psbO* transcripts from wild type and *hfp108-1*. Ten fractions of equal volume were collected from the top to bottom of 15–55% sucrose gradients, and equal proportions of the RNA purified from each fraction were analyzed by gel-blot hybridization. rRNAs were detected by ethidium bromide staining

by sucrose gradient centrifugation, prior to RNA blot analysis. The distribution of plastidic and cytosolic rRNAs in wild-type and *hfp108-1* polysome gradients showed that there was no apparent difference in the distribution of ribosomes between the wild-type and mutant plants. The distributions of the *psbA* and *psbD* mRNAs were shifted toward the top fractions of the gradient in extracts from *hfp108-1* mutants compared with extracts from wild-type plants, while the distribution of the *psbO* mRNA was not altered in the mutant (Fig. 7c).

Discussion

The chloroplast protein translation machinery is closely related to that of prokaryotes. In this study, we report the identification and characterization of the *Arabidopsis* chloroplast RRF. Our studies showed that the chloroplast RRF is involved in protein synthesis and that inactivation of this gene leads to impaired chloroplast development and embryogenesis in *Arabidopsis*.

We isolated the high chlorophyll fluorescence and pale green (*hfp*) mutant *hfp108-1* by screening the T-DNA insertion mutants with the high chlorophyll fluorescence phenotype. Through map-based cloning, the mutant locus responsible for the phenotype of *hfp108-1* was identified as *At3g63190*, which carries a repeated sequence fragment of part of sequence (including 116 nucleotides from nucleotide 631 to 746 downstream of the ATG) (Fig. 3a). This mutation led to a decreased level of *At3g63190* transcripts (Fig. 3b), which was probably due to a decreased splicing efficiency because the correctly spliced product could still be detected in *hfp108-1*. The amino acid sequence of HFP108 showed 44% amino acid identity with *E. coli* RRF (Fig. 5a), which functions in the recycling of ribosomes by splitting ribosomes into subunits and disassembling the post-termination ribosomal complexes in concert with elongation factor EF-G and initiation factor 3 (IF3)

thereby freeing the ribosome for a new round of polypeptide synthesis (Hirokawa et al. 2005). The N-terminal region of HFP108 was hypothesized to function as a transit peptide for directing the protein to the chloroplasts (Fig. 5b). These results indicate that HFP108 encodes an *Arabidopsis* chloroplast RRF orthologue, which we named AtcpRRF.

In *hfp108-1* mutants, the levels of the chloroplast-encoded proteins PsaA/B, D1 and D2 were reduced to less than 5% of the levels in wild-type plants (Fig. 6), and their transcript levels were also decreased, but ~50% of levels of the wild-type plants were detected (Fig. 7a). These results indicate that translation of the chloroplast-encoded proteins is impaired in *hfp108-1* mutants. Indeed, in vivo protein labeling experiments showed a drastic decrease in the synthesis rate of the chloroplast-encoded proteins (Fig. 7b). Analysis of the association of the chloroplast-encoded *psbA* and *psbD* mRNAs with ribosomes in the mutant showed a shift toward the top of the gradient in the ribosome loading assay. These results indicate that the protein deficiencies are due to global defects in chloroplast translation. Together, these data provide strong evidence that the AtcpRRF protein is primarily involved in translation of mRNAs from chloroplast-encoded genes. In bacteria, cooperative action of three translation factors, ribosome recycling factor (RRF), elongation factor G (EF-G), and initiation factor 3 (IF3), dissociates 70S ribosomes and remodels post-termination complexes into stable subunits. RRF and EF-G transiently split 70S ribosomes into subunits in the presence of GTP. Subsequently, the dissociation is stabilized by IF3, which binds to the transiently formed 30S subunits and prevents re-association into 70S ribosomes. The stable dissociation of ribosomes into subunits depends on the cooperation of the three factors, and the resulting subunits are ready for the next round of translation (Hirokawa et al. 2005, 2008). It is likely that the AtcpRRF protein in the chloroplast translation system functions similarly to bacterial RRF. Thus, the *hfp108-1* mutation affects the dissociation of 70S ribosomes into subunits which are ready for the next round of translation and consequently impairs the initiation of the next round of translation. However, the shift in the distribution of *psbA* and *psbD* mRNA in the polysome fractions is extremely modest compared to the sharp decrease in the translation of these mRNAs. In bacteria, besides being involved in the dissociation of 70S ribosomes into subunits (Hirokawa et al. 2005), RRF also participates in the disassembly of the post-termination complex (PoTC, which consists of ribosomes, unesterified tRNA and mRNA) into mRNA, tRNA and ribosomes (reviewed in Kaji et al. 2001; Hirokawa et al. 2006). In the absence of RRF, the ribosome is not released from the mRNA, and the upstream ribosomes remain on the mRNA (Ryoji et al. 1981a, b; Janosi et al. 1998; Hirokawa et al. 2004). The persistent association of mRNAs with polysomes might account for the very limited effect of the mutation on the polysome distribution in *hfp108-1* (Fig. 7c). These results suggest that translation elongation and termination, besides translation initiation, were perturbed in the mutant.

The steady-state levels of the nuclear-encoded *cab* and *psbO* transcripts were unaltered in the *hfp108-1* mutant; however, the protein level of PsbO was reduced. The distributions of the mutant and wild-type *psbO* mRNA in the sucrose gradients were similar between the wild-type and mutant plants (Fig. 7c). Hence, the reduction in the amounts of nuclear-encoded protein PsbO may be secondary effects of the mutational lesion. Indeed, subunits of chloroplastic protein complexes usually show concerted accumulation because the stability of the core subunits of a photosynthetic complex is generally reduced when the synthesis of the core subunits is blocked (Schmidt and Mishkind 1983; Jensen et al. 1986; Rochaix et al. 1989; Yu and Vermaas 1990, 1993). Similar situations have been reported in *apg1* mutants (Motohashi et al. 2003), *apg2* mutants (Motohashi et al. 2001), *apg3* mutants (Motohashi et al. 2007) and *apg6* mutants (Myouga et al. 2006).

RNA gel blot analysis showed a reduction in the chloroplast-encoded gene transcripts in the mutant. Changes in the chloroplast translation machinery during chloroplast development, such as a defect in rRNA processing and lesions in genes that encode ribosomal proteins or initiation factors, might modulate the stability of a subset of chloroplast mRNA molecules (Barkan 1993). Inactivation of AtcpRF2 resulted in a reduction in accumulation of the *atpE* transcripts of ~50% in the mutant, while the AtpE protein level was reduced by ~10%. In addition, the polysomal association of the *atpE* transcript was also affected (Meurer et al. 2002). Similar results have been observed in the *apg3-1* and *hcf173* mutants. In *apg3-1*, the mutant of AtcpRF1, the abnormal polysomal association of UAG-containing transcripts led to decreases in the corresponding transcripts due to the altered stability of the transcripts (Motohashi et al. 2007). The decreased ribosomal loading of the *psbA* transcript in *hcf173* affected the stability of the *psbA* transcript, thus leading to a significant reduction in the steady-state level (Schult et al. 2007). Thus, the decreased levels of chloroplast gene transcripts could be attributed to impaired ribosome recycling from the last round of translation due to the deficiency in AtcpRRF. It is also likely that translational defects affecting the expression of the subunits of plastid-encoded RNA polymerase in the *hfp108-1* mutant may be in part, responsible for the decreased accumulation of chloroplast genes transcripts, such as *psbA*, *psbB*, *psaA/B*, etc.

The *hfp108-1* mutant plastids contained much-less-abundant thylakoid membranes, which could not be

classified as grana or stroma thylakoids (Fig. 2). These results highlight the important role of the AtcpRRF protein in the normal development of thylakoid membrane structures during chloroplast biogenesis. An independent T-DNA insertion null mutant displayed an embryonic lethal phenotype (Fig. 4). Further studies showed that embryogenesis was blocked at the transition from the heart to the torpedo stage. Similarly, inactivation of RRF in vivo is bactericidal or bacteriostatic and thus RRF is essential for bacteria (Janosi et al. 1994, 1998). Loss of mitochondrial RRF in human cells has been reported to result in a reduced growth rate and cell death (Rorbach et al. 2008). The previously identified components of the chloroplast translation machinery have also been shown to be essential for embryogenesis (Albrecht et al. 2006; Motohashi et al. 2007). In fact, plastid differentiation is indeed closely related to embryonic development (Mansfield and Briarty 1991). During early embryo development, functional plastids might participate in the synthesis of metabolites that are necessary for embryonic morphogenesis. Besides AtcpRRF, there are many proteins involved in chloroplast development as well as embryonic development, such as EDD1 (Uwer et al. 1998), SCO1 (Albrecht et al. 2006; Ruppel and Hangarter 2007), RSY3 (Apuya et al. 2002), DCL (Bellaoui et al. 2003), SLP (Apuya et al. 2001), EMB506 (Albert et al. 1999), etc. They all participate in the basic biological processes of chloroplast development, e.g., composition of the protein translation machinery, ribosome stability and the transport of nuclear-encoded proteins into the chloroplast, etc. Therefore, plastid differentiation might be involved in the synthesis of metabolites that could participate in the regulation of embryonic development. However, the detailed function of plastids in embryogenesis is still not understood, i.e., the precise roles of the plastid proteins involved in regulating embryogenesis need further analysis.

The protein accession numbers used in this article are NP_567141.1 (*Arabidopsis thaliana* At3g63190), NP_0010 60047.1 (*Oryza sativa* Os07g0570700), YP_171723.1 (*Synechococcus elongatus* strain PCC6301), NP_414714.1 (*Escherichia coli* strain K-12 substrain MG1655) and NP_186829.3 (*Arabidopsis thaliana* At3g01800).

Acknowledgments We gratefully acknowledge the *Arabidopsis* Biological Resource Center for the *Arabidopsis* seeds. This research was supported by the National Natural Science Foundation of China (30725003) and National Basic Research Program of China (2009CB118500).

References

Abdallah F, Salamini F, Leister D (2000) A prediction of the size and evolutionary origin of the proteome of chloroplasts of *Arabidopsis*. Trends Plant Sci 5:141–142

Ahlert D, Ruf S, Bock R (2003) Plastid protein synthesis is required for plant development in tobacco. Proc Natl Acad Sci USA 100:15730–15735

Akkaya MS, Welsch PL, Wolfe MA, Duerr BK, Becktel WJ, Breinberger CA (1994) Purification and N-terminal sequence analysis of pea chloroplast protein synthesis factor EF-G. Arch Biochem Biophys 308:109–117

Albert S, Després B, Guilleminot J, Bechtold N, Pelletier G, Delseny M, Devic M (1999) The EMB 506 gene encodes a novel ankyrin repeat containing protein that is essential for the normal development of *Arabidopsis* embryos. Plant J 17:169–179

Albrecht V, Ingenfeld A, Apel K (2006) Characterization of the snowy cotyledon 1 mutant of *Arabidopsis thaliana*: the impact of chloroplast elongation factor G on chloroplast development and plant vitality. Plant Mol Biol 60:507–518

Apuya NR, Yadegari R, Fischer RL, Harada JJ, Zimmerman JL, Goldberg RB (2001) The *Arabidopsis* embryo mutant *schlepperless* has a defect in the chaperonin-60 alpha gene. Plant Physiol 126:717–730

Apuya NR, Yadegari R, Fischer RL, Harada JJ, Goldberg RB (2002) RASPBERRY3 gene encodes a novel protein important for embryo development. Plant Physiol 129:691–705

Barkan A (1993) Nuclear mutants of maize with defects in chloroplast polysome assembly have altered chloroplast RNA metabolism. Plant Cell 5:389–402

Barkan A (1998) Approaches to investigating nuclear genes that function in chloroplast biogenesis in land plants. Methods Enzymol 297:38–57

Bellaoui M, Keddie JS, Gruissem W (2003) DCL is a plant-specific protein required for plastid ribosomal RNA processing and embryo development. Plant Mol Biol 53:531–543

Bult CJ, White O, Olsen GJ, Zhou L, Fleischmann RD, Sutton GG, Blake JA, FitzGerald LM, Clayton RA, Gocayne JD, Kerlavage AR, Dougherty BA, Tomb JF, Adams MD, Reich CI, Overbeek R, Kirkness EF, Weinstock KG, Merrick JM, Glodek A, Scott JL, Geoghagen NS, Venter JC (1996) Complete genome sequence of the methanogenic archaeon, *Methanococcus jannaschii*. Science 273:1058–1073

Cai W, Ji D, Peng L, Guo J, Ma J, Zou M, Lu C, Zhang L (2009) LPA66 is required for editing *psbF* chloroplast transcripts in *Arabidopsis*. Plant Physiol 150:1260–1271

Campos F, Garcia-Gomez BI, Solorzano RM, Salazar E, Estevez J, Leon P, Alvarez-Buylla ER, Covarrubias AA (2001) A cDNA for nuclear-encoded chloroplast translational initiation factor 2 from a higher plant is able to complement an *infB Escherichia coli* null mutant. J Biol Chem 276:28388–28394

Chi W, Ma JF, Zhang DY, Guo JK, Chen F, Lu CM, Zhang LX (2008) The pentatricopeptide repeat protein DELAYED GREENING1 is involved in the regulation of early chloroplast development and chloroplast gene expression in *Arabidopsis*. Plant Physiol 147:573–584

Chiu W, Niwa Y, Zeng W, Hirano T, Kobayashi H, Sheen J (1996) Engineered GFP as a vital reporter in plants. Curr Biol 6:325–330

Clough SJ, Bent AF (1998) Floral dip: a simplified method for Agrobacterium-mediated transformation of *Arabidopsis thaliana*. Plant J 16:735–743

Hernandez-Torres J, Breitenberger CA, Spielmann A, Stutz E (1993) Cloning and sequencing of a soybean nuclear gene coding for a chloroplast translation elongation factor EF-G. Biochim Biophys Acta 1174:191–194

Hirashima A, Kaji A (1970) Factor dependent breakdown of polysomes. Biochem Biophys Res Commun 41:877–883

Hirokawa G, Inokuchi H, Kaji H, Igarashi K, Kaji A (2004) In vivo effect of inactivation of ribosome recycling factor-fate of ribosomes after unscheduled translation downstream of open reading frame. Mol Microbiol 54:1011–1021

Hirokawa G, Nijman RM, Raj VS, Kaji H, Igarashi K, Kaji A (2005) The role of ribosome recycling factor in dissociation of 70S ribosomes into subunits. RNA 11:1317–1328

Hirokawa G, Demeshkina N, Iwakura N, Kaji H, Kaji A (2006) The ribosome-recycling step: consensus or controversy? Trend Biochem Sci 31:143–149

Hirokawa G, Iwakura N, Kaji A, Kaji H (2008) The role of GTP in transient splitting of 70S ribosomes by RRF (ribosome recycling factor) and EF-G (elongation factor G). Nucleic Acids Res 36:6676–6687

Hirose T, Ideue T, Wakasugi T, Sugiura M (1999) The chloroplast *infA* gene with a functional UUG initiation codon. FEBS Lett 445:169–172

Ichikawa S, Kaji A (1989) Molecular cloning and expression of ribosome releasing factor. J Biol Chem 264:20054–20059

Janosi L, Shimizu I, Kaji A (1994) Ribosome recycling factor (ribosome releasing factor) is essential for bacterial growth. Proc Natl Acad Sci USA 91:4249–4253

Janosi L, Ricker R, Kaji A (1996) Dual function of ribosome recycling factor in protein biosynthesis: Disassembling the termination complex and preventing translational errors. Biochimie 78:959–969

Janosi L, Mottagui-Tabar S, Isaksson LA, Sekine Y, Ohtsubo E, Zhang S, Goon S, Nelken S, Shuda M, Kaji A (1998) Evidence for in vivo ribosome recycling, the fourth step in protein biosynthesis. EMBO J 17:1141–1151

Jensen KH, Herrin DL, Plumley FG, Schmidt GW (1986) Biogenesis of photosystem II complexes: transcriptional, translational and posttranslational regulation. J Cell Biol 103:1315–1325

Kaji A, Teyssier E, Hirokawa G (1998) Disassembly of the post-termination complex and reduction of translational error by ribosome recycling factor (RRF)-A possible new target for antibacterial agents. Biochem Biophys Res Commun 250:1–4

Kaji A, Kiel MC, Hirokawa G, Muto AR, Inokuchi Y, Kaji H (2001) The fourth step of protein synthesis: disassembly of the posttermination complex is catalyzed by elongation factor G and ribosome recycling factor, a near-perfect mimic of tRNA. Cold Spring Harb Symp Quant Biol 66:515–529

Lee KH, Kim DH, Lee SW, Kim ZH, Hwang I (2002) In vivo import experiments in protoplasts reveal the importance of the overall context but not specific amino acid residues of the transit peptide during import into chloroplasts. Mol Cells 14:388–397

Lukowitz W, Gillmor CS, Scheible WR (2000) Positional cloning in *Arabidopsis*: why it feels good to have a genome initiative working for you. Plant Physiol 123:795–806

Ma J, Peng L, Guo J, Lu Q, Lu C, Zhang L (2007) LPA2 is required for efficient assembly of photosystem II in *Arabidopsis thaliana*. Plant Cell 19:1980–1993

Mansfield SG, Briarty LG (1991) Early embryogenesis in *Arabidopsis thaliana.* II. The developing embryo. Can J Bot 69:461–476

Martínez-García JF, Monte E, Quail PH (1999) A simple, rapid and quantitative method for preparing Arabidopsis protein extracts for immunoblot analysis. Plant J 20:251–257

Meinke DW (1994) Seed development in *Arabidopsis thaliana*. In: Meyerowitz EM, Somerville CR (eds) *Arabidopsis*. Cold spring Harbor Laboratory Press, New York, pp 253–259

Meurer J, Berger A, Westhoff P (1996a) A nuclear mutant of *Arabidopsis* with impaired stability on distinct transcripts of the plastid, *psbB*, *psbD/C*, *ndhH*, and *ndhC* operons. Plant Cell 8:1193–1207

Meurer J, Meierhoff K, Westhoff P (1996b) Isolation of high-chlorophyll-fluorescence mutants of *Arabidopsis thaliana* and their characterization by spectroscopy, immunoblotting and northern hybridisation. Planta 198:385–396

Meurer J, Plücken H, Kowallik KV, Westhoff P (1998) A nuclear-encoded protein of prokaryotic origin is essential for the stability of photosystem II in *Arabidopsis thaliana*. EMBO J 17:5286–5297

Meurer J, Lezhneva L, Amann K, Gödel M, Bezhani S, Sherameti I, Oelmüller R (2002) A peptide chain release factor 2 affects the stability of UGA-containing transcripts in *Arabidopsis chloroplasts*. Plant Cell 14:3255–3269

Motohashi R, Nagata N, Ito T, Takahashi S, Hobo T, Yoshida S, Shinozaki K (2001) An essential role of a TatC homologue of DpH-dependent protein transporter in thylakoid membrane formation during chloroplast development in *Arabidopsis thaliana*. Proc Natl Acad Sci USA 98:10499–10504

Motohashi R, Ito T, Kobayashi M, Taji T, Nagata N, Asami T, Yoshida S, Yamaguchi-Shinozaki K, Shinozaki K (2003) Functional analysis of the 37-kDa inner envelope membrane polypeptide in chloroplast biogenesis, using a Ds-tagged *Arabidopsis* pale green mutant. Plant J 34:719–731

Motohashi R, Yamazaki T, Myouga F, Ito T, Ito K, Satou M, Kobayashi M, Nagata N, Yoshida S, Nagashima A, Tanaka K, Takahashi S, Shinozaki K (2007) Chloroplast ribosome release factor 1 (AtcpRF1) is essential for chloroplast development. Plant Mol Biol 64:481–497

Murashige T, Skoog F (1962) A revised medium for rapid growth and bioassays with tobacco tissue cultures. Physiol Plant 15:473–497

Myouga F, Motohashi R, Kuromori T, Nagata N, Shinozaki K (2006) An *Arabidopsis* chloroplast-targeted Hsp101 homologue, APG6, has an essential role in chloroplast development as well as heat-stress response. Plant J 48:249–260

Peng L, Ma J, Chi W, Guo J, Zhu S, Lu Q, Lu C, Zhang L (2006) LOW PSII ACCUMULATION1 is involved in efficient assembly of photosystem II in *Arabidopsis thaliana*. Plant Cell 18:955–969

Pih KT, Yi MJ, Liang YS, Shin BJ, Cho MJ, Hwang I, Son D (2000) Molecular cloning and targeting of a fibrillarin homolog from *Arabidopsis*. Plant Physiol 123:51–58

Rochaix JD (1996) Post-transcriptional regulation of chloroplast gene expression in *Chlamydomonas reinhardtii*. Plant Mol Biol 32:327–341

Rochaix JD, Kuchka M, Mayfield S, Schirmer-Rahire M, Girard-Bascou J, Bennoun P (1989) Nuclear and chloroplast mutations affect the synthesis or stability of the chloroplast *psb*C gene product in *Chlamydomonas reinhardtii*. EMBO J 8:1013–1021

Rolland N, Janosi L, Block MA, Teyssier E, Miége C, Chéniclet C, Carde J-P, Kaji A, Joyard J (1999) Plant ribosome recycling factor homologue is a chloroplastic protein and is bactericidal in *Escherichia coli* carrying temperature-sensitive ribosome recycling factor. Proc Natl Acad Sci USA 96:5464–5469

Rorbach J, Richter R, Wessels HJ, Wydro M, Pekalski M, Farhoud M, Kühl I, Gaisne M, Bonnefoy N, Smeitink JA, Lightowlers RN, Chrzanowska-Lightowlers ZM (2008) The human mitochondrial ribosome recycling factor is essential for cell viability. Nucleic Acids Res 36:5787–5799

Ruppel NJ, Hangarter RP (2007) Mutations in a plastid-localized elongation factor G alter early stages of plastid development in *Arabidopsis thaliana*. BMC Plant Biol 7:37

Ryoji M, Berland R, Kaji A (1981a) Reinitiation of translation from the triplet next to the amber termination codon in the absence of ribosome-releasing factor. Proc Natl Acad Sci USA 78:5973–5977

Ryoji M, Karpen JW, Kaji A (1981b) Further characterization of ribosome releasing factor and evidence that it prevents ribosomes from reading through a termination codon. J Biol Chem 256:5798–5801

Sambrook J, Russell DW (2001) Molecular clone, a laboratory manual. Cold Spring Harbor Laboratory Press, New York

Sato S, Nakamura Y, Kaneko T, Asamizu E, Tabata S (1999) Complete structure of the chloroplast genome of *Arabidopsis thaliana*. DNA Res 6:283–290

Schmidt G, Mishkind N (1983) Rapid degradation of unassembled ribulose 1, 5-bisphosphate carboxylase small subunits in chloroplasts. Proc Natl Acad Sci USA 80:2632–2636

Schult K, Meierhoff K, Paradies S, Töller T, Wolff P, Westhoff P (2007) The Nuclear-encoded factor HCF173 is involved in the initiation of translation of the *psbA* mRNA in *Arabidopsis thaliana*. Plant Cell 19:1329–1346

Sugita M, Sugiura M (1996) Regulation of gene expression in chloroplasts of higher plants. Plant Mol Biol 32:315–326

Sugiura M (1992) The chloroplast genome. Plant Mol Biol 19:149–168

Uwer U, Willmitzer L, Altmann T (1998) Inactivation of a glycyl-tRNA synthetase leads to an arrest in plant embryo development. Plant Cell 10:1277–1294

Weigel D, Ahn JH, Blázquez MA, Borevitz JO, Christensen SK, Fankhauser C, Ferrándiz C, Kardailsky I, Malancharuvil EJ, Neff MM, Nguyen JT, Sato S, Wang Z, Xia Y, Dixon RA, Harrison MJ, Lamb CJ, Yanofsky MF, Chory J (2000) Activation tagging in *Arabidopsis*. Plant Physiol 122:1003–1014

Yu J, Vermaas W (1990) Transcript levels and synthesis of photosystem II components in cyanobacterial mutants with inactivated photosystem II genes. Plant Cell 2:315–322

Yu J, Vermaas W (1993) Synthesis and turnover of photosystem II reaction centre polypeptides in cyanobacterial D2 mutants. J Biol Chem 268:7407–7413

Zerges W (2000) Translation in chloroplasts. Biochimie 82:583–601